Cent. Eur. J. Geosci. • 4(2) • 2012 • 261-274
DOI: 10.2478/s13533-011-0050-2

VERSITA

Central European Journal of **Geosciences**

Fluid inclusion studies in datolite of low grade metamorphic origin from a Jurassic pillow basalt series in northeastern Hungary

Research Article

Gabriella Kiss[1]*, Ferenc Molnár[1] and Federica Zaccarini[2]

1 *Department of Mineralogy, Eötvös Loránd University, Budapest 1117, Pázmány P. stny 1/c, Hungary*

2 *Department of Applied Geosciences and Geophysics, University of Leoben, Leoben 8700, Peter Tunner Str. 5, Austria*

Received 12 October 2011; accepted 21 December 2011

Abstract: The Jurassic pillow basalt blocks in the Szarvaskő Unit in the SW-Bükk Mountains are incorporated into an accretionary mélange of Cretaceous age which had been displaced from the Dinarides to NE-Hungary during the Alpine-Carpathian collision. The pillow basalt series is a part of an incomplete remnant of an ophiolite-like sequence from which ultramafic units and sheeted dikes are almost completely absent. At the studied Egerbakta quarry, closely packed pillow, pillow fragmented hyaloclastite breccia and peperitic facies of submarine basaltic volcanism were recognized. Peperitic facies was formed by local admixture of unconsolidated siliciclastic sediment into the basaltic lava. Basaltic pillows contains short and thin prehnite-chlorite-carbonate-quartz veins formed during the interaction of seawater with the cooling lava, as well as cross-cutting datolite-prehnite-quartz-chlorite-albite bearing veins. Calcite in the short cooling cracks crystallised from upheated seawater at around 160°C temperature and 0.5-0.6 kbar pressure (water depth of about 5-6 km). Datolite precipitations in veins can be classified into at least three different textural-morphological types but all of them contain methane bearing primary fluid inclusion assemblages, with variable methane/water ratios, suggesting an inhomogeneous entrapment from a heterogeneous aqueous-carbonic fluid. End member primary fluid inclusions contain aqueous liquid with methane rich vapour phase and apparently methane only inclusions characterized by liquid phase on room temperature. A combination of results from fluid inclusion microthermometry, Raman spectroscopy (used not only for phase identification but also for determination of salinities) and temperatures calculated from chlorite compositions, show that the precipitation of datolite had taken place from low salinity (0.2-2 NaCl equiv. mass%) aqueous-methane fluids under increasing temperature and pressure (from 160 to 210°C, and from 0.6 to 1.1 kbar) conditions. The elevated pressures and temperatures in comparison to the submarine hydrothermal processes suggest that the datolite bearing mineral parageneses had been formed during the progression of Alpine very low grade metamorphic processes.

Keywords: datolite • fluid inclusions • Raman spectroscopy • pillow basalt • Alpine metamorphism

*E-mail: gabriella-kiss@chello.hu

1. Introduction

The pillow basalt blocks of Jurassic age occurring in the Szarvaskő Unit of the Bükk Mts. in northeastern Hungary bear not only the effects of submarine hydrothermal alteration [1], but also the results of the very low-grade to low-grade regional Alpine metamorphism [2–4]. Both processes resulted in aboundant veinlets. The mineralization in cooling cracks of pillows and matrix of hyaloclastite breccia has been formed during the submarine hydrothermal, while the longer cross-cutting veins have been resulted from superimposing fluid flow processes. In one of the pillow basalt outcrops, in a quarry near Egerbakta village, occurrence of datolite ($CaBSiO_4(OH)$) was discovered [5] in the latter type of veins. This is so far the only known occurrence of datolite in Hungary. In general, it is believed that datolite is a relatively low-temperature hydrothermal mineral, however, it is known from skarns, too, and rare occurrences in regionally metamorphosed rocks have also been reported [6, 7]. Due to the rarity of well-crystalline datolite, no extended fluid inclusion data base is available for this mineral. Therefore our work aims to contribute knowledge about formation conditions of this mineral by results of fluid inclusion petrography, microthermometry, Raman spectroscopy and mineral chemistry studies. In the current paper we show that datolite was formed during low grade metamorphic processes in that part of the studied basaltic unit where siliciclastic sediments are admixed to the pillow lavas.

2. Geological setting

The Szarvaskő Unit is a part of the Bükk Unit, within the Pelso Composite Unit of the Alpine Carpathian Pannonian Terrane (ALCAPA, Fig. 1A). The approximately 25 km^2-large area of the Szarvaskő Unit with outcrops of predominantly basaltic and gabbroic rocks is interpreted to be a part of the nappe system of the Bükk Unit. The lowest unit in this nappe system is the "Bükk Parautochton" which contains Paleozoic to Jurassic sedimentary formations, whereas the covering Mónosbél Unit consists of mainly Jurassic redeposited slope sediments. The Szarvaskő Unit which is overthrusted on the Mónosbél Unit is an incomplete Jurassic ophiolite-like sequence associated with deep-sea sediments. The uppermost Darnó Unit consists of Triassic and Jurassic submarine volcanites and related sediments (Fig. 1B) [8–10].

The magmatic sequence of the Szarvaskő Unit is quite uncommon in comparison to well-known ophiolites because the mantle section with harzburgitic-lherzolitic ultramafic units and sheeted dikes are absent. Cumulate gabbro is

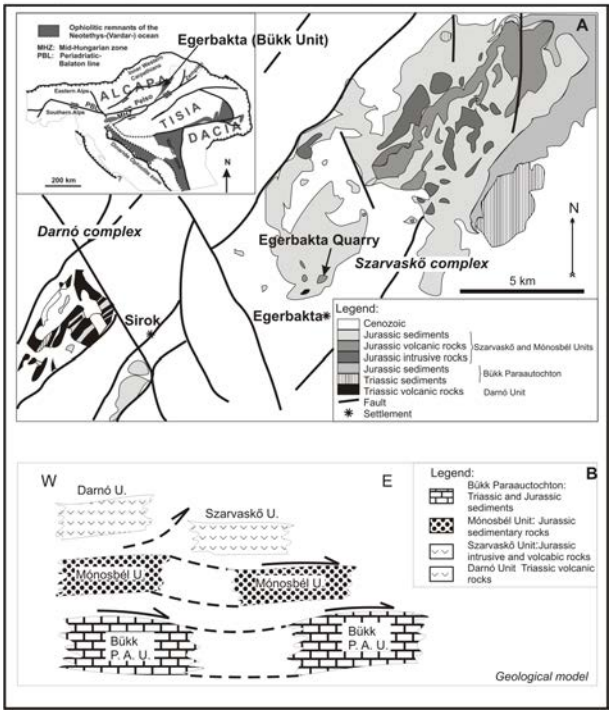

Figure 1. Simplified pre-Tertiary geological map **(A)** and tectonic reconstruction model **(B)** of the Bükk Unit (slightly modified after [10]). The studied locality, Egerbakta, is also shown.

abundant and it is rarely accompanied by very small ultramafic bodies (hornblendite, Fe-Ti-rich wehrlite). The upper part of the plutonic-volcanic sequence with various gabbroic and related plagiogranitic rocks and pillow basalt flows is well preserved, though they are strongly tectonised. These magmatic rocks are hosted by an accretionary mélange series in a form of up to several kilometre large blocks in olistolithic turbiditic shales, slates and sandstones of Jurassic age, but gabbro-sediment contacts with contact-metamorphic recrystallization also occurs [11–13].

The petrochemical data for the mafic-ultramafic rocks of the Szarvaskő Unit show some significant differences from MORB composition and a back-arc-basin or a marginal sea setting has been suggested as the environment of their formation [14–17]. According to the current geotectonic models the formation of this unit took place in a Middle-Late Jurassic back-arc-basin within the Vardar Ocean, in the northwesternmost segment of the Neo-Tethys. The recent setting in a mélange in NE-Hungary is due to the Late Jurassic/Early Cretaceous subduction/collision related accretionary prism formation, and a later, Tertiary displacement from the Dinarides along the Mid-Hungarian Lineament [12, 13, 18, 19]. The radiometric age of the gabbro of the Szarvaskő Unit is 166±8 Ma [20],

which is comparable with the ages obtained from ophiolitic rocks of the Dinaridic Ophiolites and also partly of the Vardar Ophiolites [18, 21].

The pillow basalt blocks of the Szarvaskő Unit show the results of a quite limited seawater-rock hydrothermal interaction. This interaction resulted in the albitization of plagioclase, the formation of chlorite in the ground mass and precipitation of hydrothermal quartz, prehnite, chlorite and calcite in short cooling cracks of the basalt pillows and in the matrix of the inter-pillow hyaloclastite breccia [1]. Cross cutting veins with prehnite, chlorite, quartz, calcite and feldspar occur not only in the basalt pillow sequence, but also in the gabbro intrusions. These veins are the results of an early Alpine, very low-grade metamorphism [2, 22]. This metamorphism took place between the eo-Hellenic (160-120 Ma, Dinaridic subduction related) and the Austrian (100-95 Ma, compressional crustal thickening related) phases [3] and it was a low temperature, anchizonal to epizonal event corresponding to prehnite-pumpelleyite facies with illite-muscovite K/Ar ages of about 120 Ma [4, 19]. Its maximum reached a temperature of 270-285°C and a pressure of 1.5-2 kbar, in the southwestern part of the Bükk Mts. [22].

3. Analytical methods

Conventional petrography of host rock and vein samples was followed by fluid inclusion study. The fluid inclusion petrography and microthermometric study were carried out on 80-100 µm thick double polished sections using a Linkam FT-IR 600 type heating-freezing stage mounted on an Olympus BX-51 type polarizing microscope providing up to 1000 times optical magnification. The calibration of the stage was made by microthermometric measurements on H_2O-CO_2 and pure water synthetic fluid inclusions. The precision of the microthermometric measurements was ±0.1°C below 0°C, and ±1°C above it. Interpretation of the microthermometric data was carried out by a programme developed in the Visual Basic environment by the first author using the equations of [23–26], while the methane isochor calculations were done using the equation of state of [27] included in the FLINCOR software of [28]. The results were also checked with the help of the softwares ISOC and BULK [29]. Raman microanalyses of fluid inclusions in datolite were completed using a Horiba Yvon Jobin LabRAM HR 800 edge filter based confocal dispersive Raman spectrometer, 800 mm focal length, coupled with an Olympus BXFM type microscope at the Eötvös Loránd University, Budapest. During the measurements, 532 nm emission of a frequency doubled Nd:YAG laser, 600 grooves/mm grating, 50 µm confocal aperture and 50x long working distance objective were used. For some measurements the Linkam FTIR 600 microthermometric stage was mounted to the spectrometer and analyses were performed at different temperatures.

Mineral chemistry of datolite was analyzed by a Superprobe Jeol JXA 8200 electron microprobe at the Eugen F. Stumpfl Laboratory, University of Leoben. The electron microprobe was operated in the wawelength dispersive mode, with 15 kV accelerating voltage and 10 nA beam current. The detectation limits were 100 ppm for Cl, Na, Al, Si, K and Ca, while B and F have a detection limit of 2000 ppm. Electron microprobe analysis of the chlorite cogenetic with datolite was completed in the EPMA Laboratory of the Masaryk University, Brno by means of a CAMECA SX 100 type instrument (15 kv accelerating potential, a beam current of 10 nA and a beam size of 4µm). The detection limits were 600 ppm for Na, 400 ppm for Si and V, 350 ppm for Al, 450 ppm for Mg and K, 300 ppm for Ca, Cr, Cl and Ti, 1200 ppm for Ba, 800 ppm for Fe and Ni, 700 ppm for Mn and F and 2000 ppm for Zn.

4. Results

4.1. Mineralogy and petrography of the veins and their host rock

The Egerbakta quarry is situated about 8 km NW of the town of Eger in northeast Hungary. The quarry exposes mainly blocks of closely packed pillow lava, but in its northwestern part the so-called peperitic facies *s.l.* (i.e. local admixture of unconsolidated siliciclastic sediment at the time of basalt eruption) and a small block of pillow fragmented hyaloclastite breccia also occurs [1].

The less altered basalt shows porphyry intersertal texture, where the plagioclase and augite occur as groundmass minerals with <0.4 mm and as phenocrysts with up to 2 mm sizes. However, the fine grained chloritic matrix and albitic composition of plagioclase indicate submarine hydrothermal alteration. The former siliciclastic sediment is now completely altered to hydrothermal minerals, mainly to quartz and albite. At present only the preserved texture indicate the sedimentary origin of that rock.

Other hydrothermal minerals, such as quartz, calcite, chlorite and prehnite occur in short, 2-4 mm thin cooling cracks which terminate within or at the boundaries of the pillows and as the cementing matrix of hyaloclastite breccia. No alteration halo is observed along the wall of the anhedral crystal bearing veins. The mode of appearance of this kind of mineralization also suggests its formation during the hydrothermal processes associated with cooling of basalt in every volcanic facies. Compositions of chlorite in para-

geneses with the minerals of the short cooling cracks and chlorite occuring as hydrothermal alteration mineral in the ground mass of the basalt were analyzed by electronmicroprobe (Table 1). The results of all chlorites correspond to Type 1, Mg-chlorite according to [30], with Al(IV) values between 0.69-0.89 and XFe values between 0.41-0.60, respectively.

Prehnite, calcite, quartz, chlorite and albite occur in up to several meters long veins with up to 3 cm thicknesses cross-cutting the closely packed pillow and pillow fragmented hyaloclastite breccia facies. Datolite exclusively appears in these extensive veins where they are cutting the peperitic basalt facies (Fig. 2**A**). Datolite bearing veins are cut by short and thin (0.3-1 mm) veinlets with very fine grained milky cacite.

Euhedral to subhedral prehnite with anhedral quartz-calcite-prehnite-albite assemblage occur along the walls of the datolite bearing veins. Anhedral datolite usually fills up spaces among these crystals, however, more spectacular euhedral crystals of datolite are also present in several centimetre large elongated open spaces of veins. The size of the euhedral datolite crystals reach up to 1 cm (Fig. 2**B**). Though precise crystal face indexing by optical goniometer was not performed, the stereomicroscopic observations support classifiaction of euhedral datolite crystals into "type 4" and "type 8" groups (with occurrence of more prismatic and more isometric varieties), according to [31]. Datolite closer to the walls of the vein is dull, or spongy, due to the presence of large amount of fluid inclusions whereas it is water-clear (i.e. only a few inclusions occur) in the central parts of the open spaces (Fig. 2**C**). The transitional zones between these two textural groups are subdivided into spongy-transitional and water-clear-transitional subtypes. In the inner parts of the vein, anhedral chlorite, prehnite, calcite and albite occur rarely together with the datolite.

Along the datolite-bearing veins a 2-5 cm thick zone of the basalt is more strongly altered (Fig. 2**D**) compared to the generally present hydrothermal alteration (Fig. 2**E**). Fine grained prehnite, clay minerals and chlorite replace the matrix, whereas the rock forming phenocrysts are completely pseudomorphosed by prehnite and chlorite in this alteration halo.

Results of electron microprobe analysis of datolite revealed that there is no significant systematically occuring compositional difference among the spongy, transitional and water-clear, as well as anhedral and euhedral varieties (Table 2). All of them consist of typical datolite constituents (Ca, B, and Si) with minor Al, K, Na, F and Cl contents. F and Cl are present as substitution of the OH group [6, 7]. Cl contents of analysed crystals are rarely higher than the detection limit of the electronmicroprobe, however, F occur with highly variable and up to 0.75 wt.% concentrations.

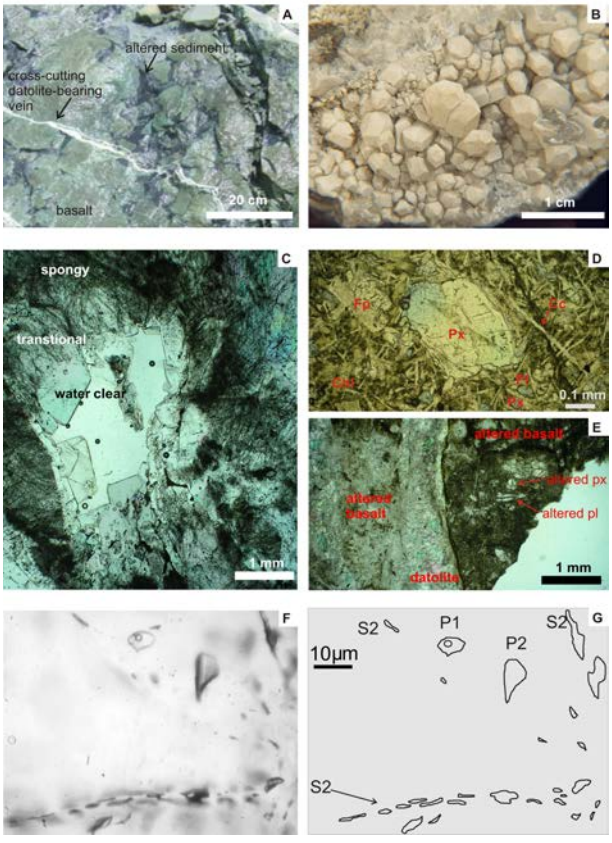

Figure 2. **A** A siliciclastic peperitic block in the Egerbakta quarry with cross-cutting datolite-bearing vein. **B** Euhedral datolite in the drusy part of the vein shown on Fig. **2A**. The habit of crystals corresponds to'type 4' in the system of [31]. **C** Spongy, transitional and water-clear datolite in thin section (1N). **D** Porphyry intersertal basalt far from the datolite-bearing veins. Hydrothermal alteration product chlorite occurs in the matrix, while calcite in a short veinlet (cooling crack) also can be found (1N). **E** Strongly altered basalt next to the datolite-bearing vein (1N). **F-G** Primary aqueous liquid rich (P1) and liquid methane rich (P2) inclusions in water-clear datolite forming an assemblage, occurring far from healed microfractures filled with secondary inclusions (S2).
Used abbreviations: cc: calcite; chl: chlorite; fp: feldspar; pl: plagioclase; px: pyroxene.

The results of electronmicroprobe analysis of chlorite occurring together with the water-clear datolite (Table 1) show that compositions correspond to "type 1" Mg-chlorites [30], i.e. brunsvigites. The calculated Al (IV) values are between 0.98-1.05, while XFe values are between 0.45-0.49.

Table 1. Representative results of electron microprobe analyses of chlorite.

	Chlorite in cooling cracks	Chlorite in the groundmass of the basalt							Chlorite occuring together with transitional datolite						
	1.	2.	3.	4.	5.	6.	7.	*average*	1.	2.	3.	4.	5.	6.	*average*
SiO_2	30.97	29.98	28.23	28.07	28.21	28.39	29.47	*28.73*	28.03	29.39	28.27	27.26	28.57	28.18	*28.28*
TiO_2	0.04	0.03	0.04	0.06	0.03	0.06	0.02	*0.04*	b.d.l.	0.01	b.d.l.	b.d.l.	b.d.l.	0.03	*0.02*
Al_2O_3	16.58	16.00	14.66	14.29	14.75	14.53	16.25	*15.08*	16.78	17.45	16.99	16.93	17.32	16.73	*17.03*
Cr_2O_3	b.d.l.	0.01	0.05	b.d.l.	b.d.l.	b.d.l.	0.03	*0.03*	b.d.l.	b.d.l.	0.02	0.01	b.d.l.	0.01	*0.01*
FeOT	19.55	26.29	30.41	26.24	30.92	26.43	25.65	*27.66*	26.69	25.96	26.07	26.53	25.01	26.14	*26.07*
MnO	0.31	0.36	0.66	0.37	0.54	0.52	0.45	*0.48*	0.27	0.3	0.31	0.36	0.35	0.31	*0.32*
MgO	9.54	14.59	10.80	12.19	10.66	12.21	15.13	*12.60*	15.13	16.4	15.58	14.97	16.73	15.99	*15.80*
CaO	8.23	0.48	0.63	0.95	0.69	1.14	0.32	*0.70*	0.14	0.14	0.13	0.11	0.27	0.18	*0.16*
Na_2O	n.a.	n.a.	n.a.	n.a.	n.a.	n.a.	n.a.	*n.a.*	b.d.l.	0.04	0.06	0.03	0.02	0.02	*0.03*
K_2O	0.04	0.03	0.03	0.04	0.02	0.05	b.d.l.	*0.03*	0.01	0.02	0.03	0.01	0.03	0.03	*0.02*
V_2O_3	n.a.	n.a.	n.a.	n.a.	n.a.	n.a.	n.a.	*n.a.*	0.02	0.03	0.03	0.02	0.03	0.01	*0.02*
NiO	n.a.	n.a.	n.a.	n.a.	n.a.	n.a.	n.a.	*n.a.*	b.d.l.	0.07	0.01	0.01	b.d.l.	b.d.l.	*0.03*
ZnO	n.a.	n.a.	n.a.	n.a.	n.a.	n.a.	n.a.	*n.a.*	0.13	0.07	0.02	0.03	b.d.l.	b.d.l.	*0.06*
Cl	0.01	b.d.l.	b.d.l.	0.03	0.01	0.01	b.d.l.	*0.02*	b.d.l.	b.d.l.	0.02	b.d.l.	b.d.l.	0.01	*0.02*
F	n.a.	n.a.	n.a.	n.a.	n.a.	n.a.	n.a.	*n.a.*	b.d.l.	b.d.l.	b.d.l.	b.d.l.	b.d.l.	b.d.l.	b.d.l.
Total	*85.27*	87.77	85.51	82.24	85.83	83.34	87.32	*85.34*	*87.2*	*89.88*	*87.54*	*86.27*	*88.33*	*87.64*	*87.81*
	Calculated cation numbers (14 oxygene)														
Si (IV)	3.31	3.16	3.15	3.20	3.15	3.19	3.11	*3.16*	2.99	3.02	3.00	2.95	2.98	2.98	*2.99*
Al (IV)	0.69	0.84	0.85	0.80	0.85	0.81	0.89	*0.84*	1.01	0.98	1.00	1.05	1.02	1.02	*1.01*
Total (IV)	4.00	4.00	4.00	4.00	4.00	4.00	4.00	*4.00*	*4.00*	*4.00*	*4.00*	*4.00*	*4.00*	*4.00*	*4.00*
Al (VI)	1.40	1.15	1.09	1.11	1.09	1.12	1.14	*1.11*	1.11	1.13	1.12	1.11	1.11	1.07	*1.11*
Ti	0.00	0.00	0.00	0.01	0.00	0.01	0.00	*0.00*	b.d.l.	0.00	b.d.l.	b.d.l.	b.d.l.	0.00	*0.00*
Cr	0.00	0.00	0.00	b.d.l.	b.d.l.	b.d.l.	0.00	*0.00*	b.d.l.	b.d.l.	0.00	0.00	b.d.l.	0.00	*0.00*
Fe	1.75	2.32	2.84	2.50	2.88	2.48	2.27	*2.55*	2.38	2.23	2.31	2.40	2.18	2.32	*2.30*
Mn	0.03	0.03	0.06	0.04	0.05	0.05	0.04	*0.05*	0.02	0.03	0.03	0.03	0.03	0.03	*0.03*
Mg	1.52	2.29	1.80	2.07	1.77	2.05	2.38	*2.06*	2.41	2.51	2.46	2.41	2.60	2.52	*2.49*
Ca	0.94	0.05	0.08	0.12	0.08	0.14	0.04	*0.08*	0.02	0.02	0.01	0.01	0.03	0.02	*0.02*
K	0.01	0.00	0.00	0.01	0.00	0.01	b.d.l.	*0.00*	0.00	0.00	0.00	0.00	0.00	0.00	*0.00*
Na	n.a.	n.a.	n.a.	n.a.	n.a.	n.a.	n.a.	*n.a.*	0.00	0.01	0.01	0.01	0.00	0.00	*0.01*
V	n.a.	n.a.	n.a.	n.a.	n.a.	n.a.	n.a.	*n.a.*	0.00	0.00	0.00	0.00	0.00	0.00	*0.00*
Ni	n.a.	n.a.	n.a.	n.a.	n.a.	n.a.	n.a.	*n.a.*	b.d.l.	0.01	0.00	0.00	b.d.l.	b.d.l.	*0.00*
Zn	n.a.	n.a.	n.a.	n.a.	n.a.	n.a.	n.a.	*n.a.*	0.02	0.01	0.00	0.00	b.d.l.	b.d.l.	*0.01*
Total (VI)	*5.65*	5.85	5.88	5.84	5.88	5.84	5.87	*5.86*	*5.96*	*5.94*	*5.95*	*5.98*	*5.96*	*5.97*	*5.96*
vacancy	0.36	0.15	0.12	0.16	0.12	0.16	0.13	*0.14*	0.04	0.06	0.05	0.02	0.04	0.03	*0.04*
XFe	0.41	0.49	0.59	0.53	0.60	0.53	0.48	*0.54*	0.49	0.46	0.48	0.49	0.45	0.47	*0.48*
Cl	0.00	b.d.l.	b.d.l.	0.04	0.00	0.00	b.d.l.	*0.01*	b.d.l.	b.d.l.	0.01	b.d.l.	b.d.l.	0.00	*0.01*
F	n.a.	n.a.	n.a.	n.a.	n.a.	n.a.	n.a.	*n.a.*	b.d.l.	b.d.l.	b.d.l.	b.d.l.	b.d.l.	b.d.l.	b.d.l.
Mg+Fe total	3.27	4.61	4.64	4.57	4.66	4.53	4.65	*4.61*	4.79	4.74	4.77	4.81	4.78	4.84	*4.79*
Al+vacancy	1.75	1.30	1.21	1.27	1.20	1.27	1.27	*1.25*	1.14	1.19	1.16	1.13	1.15	1.10	*1.14*
	Classification (Zane and Weiss, 1998)														
Type	Type 1	Type 1	Type 1	Type 1	Type 1	Type 1	Type 1		Type 1	Type 1	Type 1	Type 1	Type 1	Type 1	
Name	Mg-chlorite	Mg-chlorite	Mg-chlorite	Mg-chlorite	Mg-chlorite	Mg-chlorite	Mg-chlorite		Mg-chlorite	Mg-chlorite	Mg-chlorite	Mg-chlorite	Mg-chlorite	Mg-chlorite	
	Calculated crystallisation temperature (Zang and Fyfe, 1995)														
°C	157	182	173	171	174	172	192	*177*	217	215	218	227	224	221	*220*

4.2. Fluid inclusions

Fluid inclusion studies were performed in calcite from the short cooling cracks of pillow basalt (Fig. 2**D**) and in datolite from the more extended cross-cutting veins (Fig. 2**C**,**E**).

Calcite from the cooling cracks contains 5-20 μm large aqueous liquid-vapor primary fluid inclusions. These inclusions occur isolated or in clusters of 5-8 small inclusions apart from the healed microcracks and they were found in the rarely observable growth zones of calcite

Table 2. Representative results of electron microprobe analyses of datolite.

		B_2O_3	Al_2O_3	Cl	SiO_2	CaO	F	Na_2O	K_2O	Total	B	Al	Cl	Si	Ca	F	Na	K	Calculated cation numbers (4 oxygene)		
																			Ca	B	Si
Spongy datolite	1.	21.89	b.d.l.	b.d.l.	37.40	33.94	b.d.l.	b.d.l.	b.d.l.	93.23	6.80	b.d.l.	b.d.l.	17.48	24.25	b.d.l.	b.d.l.	b.d.l.	0.97	1.01	1.00
	2.	22.52	0.01	b.d.l.	37.15	33.98	b.d.l.	0.01	b.d.l.	93.67	6.99	0.00	b.d.l.	17.37	24.29	b.d.l.	0.01	b.d.l.	0.97	1.03	0.99
	3.	22.52	0.03	b.d.l.	37.07	34.05	0.62	0.01	b.d.l.	94.03	6.99	0.02	b.d.l.	17.33	24.33	0.62	0.00	b.d.l.	0.97	1.03	0.99
	4.	23.58	b.d.l.	b.d.l.	37.01	33.83	b.d.l.	b.d.l.	b.d.l.	94.42	7.32	b.d.l.	b.d.l.	17.30	24.18	b.d.l.	b.d.l.	b.d.l.	0.97	1.08	0.99
	5.	21.88	0.04	b.d.l.	37.49	34.06	b.d.l.	0.02	b.d.l.	93.50	6.80	0.02	b.d.l.	17.53	24.34	b.d.l.	0.02	b.d.l.	0.97	1.01	1.00
	6.	22.03	b.d.l.	b.d.l.	37.26	33.86	0.71	b.d.l.	b.d.l.	93.56	6.84	b.d.l.	b.d.l.	17.42	24.20	0.71	b.d.l.	b.d.l.	0.97	1.01	0.99
	7.	22.19	b.d.l.	b.d.l.	37.27	33.96	b.d.l.	b.d.l.	b.d.l.	93.48	6.89	b.d.l.	b.d.l.	17.42	24.27	b.d.l.	b.d.l.	b.d.l.	0.97	1.02	0.99
	8.	23.20	0.05	b.d.l.	36.97	34.02	b.d.l.	0.02	b.d.l.	94.29	7.20	0.03	b.d.l.	17.28	24.32	b.d.l.	0.02	b.d.l.	0.97	1.07	0.98
	9.	23.09	b.d.l.	0.01	37.06	34.13	b.d.l.	b.d.l.	b.d.l.	94.29	7.17	b.d.l.	0.01	17.32	24.39	b.d.l.	b.d.l.	b.d.l.	0.97	1.06	0.99
	Average	*22.55*	*0.03*	*0.01*	*37.19*	*33.98*	*0.66*	*0.02*	*b.d.l.*	*93.83*	*7.00*	*0.02*	*0.01*	*17.38*	*24.29*	*0.66*	*0.01*	*b.d.l.*	*0.97*	*1.04*	*0.99*
Transitional datolite	1.	22.57	0.03	b.d.l.	37.33	33.87	b.d.l.	0.01	0.01	93.82	7.01	0.02	b.d.l.	17.45	24.20	b.d.l.	0.01	0.01	0.97	1.04	0.99
	2.	21.76	0.01	0.02	37.48	34.21	0.05	0.03	0.01	93.55	6.76	0.00	0.02	17.52	24.45	0.05	0.02	0.01	0.98	1.00	1.00
	3.	22.63	b.d.l.	0.02	37.37	34.20	b.d.l.	b.d.l.	b.d.l.	94.22	7.03	b.d.l.	0.02	17.47	24.44	b.d.l.	b.d.l.	b.d.l.	0.98	1.04	0.99
	4.	22.08	0.04	b.d.l.	37.13	33.93	0.29	b.d.l.	0.01	93.36	6.86	0.02	b.d.l.	17.36	24.25	0.29	b.d.l.	0.01	0.97	1.01	0.99
	5.	23.82	0.03	0.01	37.06	33.99	b.d.l.	b.d.l.	b.d.l.	94.92	7.40	0.01	0.01	17.33	24.29	b.d.l.	b.d.l.	b.d.l.	0.97	1.09	0.99
	6.	23.23	0.06	b.d.l.	36.90	34.11	0.05	0.01	b.d.l.	94.33	7.21	0.03	b.d.l.	17.25	24.38	0.05	0.01	b.d.l.	0.97	1.07	0.98
	7.	23.19	0.06	0.02	36.89	34.17	0.05	b.d.l.	b.d.l.	94.35	7.20	0.03	0.02	17.24	24.42	0.05	b.d.l.	b.d.l.	0.97	1.07	0.98
	8.	22.49	b.d.l.	b.d.l.	37.18	33.97	b.d.l.	b.d.l.	b.d.l.	93.63	6.98	b.d.l.	b.d.l.	17.38	24.28	b.d.l.	b.d.l.	b.d.l.	0.97	1.03	0.99
	9.	23.08	0.01	b.d.l.	37.24	34.05	0.75	b.d.l.	b.d.l.	94.82	7.17	0.01	b.d.l.	17.41	24.33	0.75	b.d.l.	b.d.l.	0.97	1.06	0.99
	10.	22.17	b.d.l.	b.d.l.	37.29	34.05	b.d.l.	0.02	0.02	93.55	6.89	b.d.l.	b.d.l.	17.43	24.34	b.d.l.	0.01	0.01	0.97	1.02	0.99
	11.	21.37	0.04	0.01	37.53	34.12	b.d.l.	0.04	0.03	93.13	6.63	0.02	0.01	17.54	24.38	b.d.l.	0.03	0.02	0.97	0.98	1.00
	12.	22.65	b.d.l.	0.02	37.56	34.11	b.d.l.	0.01	b.d.l.	94.35	7.03	b.d.l.	0.02	17.56	24.38	b.d.l.	0.00	b.d.l.	0.97	1.04	1.00
	Average	*22.59*	*0.03*	*0.02*	*37.25*	*34.06*	*0.24*	*0.02*	*0.01*	*94.00*	*7.01*	*0.02*	*0.02*	*17.41*	*24.35*	*0.24*	*0.01*	*0.01*	*0.97*	*1.04*	*0.99*
Water-clear datolite	1.	22.77	b.d.l.	b.d.l.	37.25	34.06	b.d.l.	b.d.l.	b.d.l.	94.08	7.07	b.d.l.	b.d.l.	17.41	24.34	b.d.l.	b.d.l.	b.d.l.	0.97	1.05	0.99
	2.	22.40	b.d.l.	b.d.l.	36.89	33.85	0.85	0.01	b.d.l.	93.64	6.95	b.d.l.	b.d.l.	17.24	24.19	0.85	0.01	b.d.l.	0.97	1.03	0.98
	3.	23.79	b.d.l.	0.01	37.28	33.82	0.05	0.01	0.01	94.94	7.39	b.d.l.	0.01	17.43	24.17	0.05	0.00	0.01	0.96	1.09	0.99
	4.	23.03	b.d.l.	0.01	37.03	34.11	0.34	0.02	b.d.l.	94.38	7.15	b.d.l.	0.01	17.31	24.38	0.34	0.01	b.d.l.	0.97	1.06	0.99
	5.	23.89	b.d.l.	b.d.l.	36.91	33.83	b.d.l.	0.02	b.d.l.	94.64	7.42	b.d.l.	b.d.l.	17.25	24.18	b.d.l.	0.01	b.d.l.	0.97	1.10	0.98
	6.	23.23	b.d.l.	b.d.l.	37.15	34.05	0.29	b.d.l.	0.01	94.61	7.22	b.d.l.	b.d.l.	17.37	24.33	0.29	b.d.l.	0.00	0.97	1.07	0.99
	Average	*23.18*	*b.d.l.*	*0.01*	*37.08*	*33.95*	*0.38*	*0.01*	*0.01*	*94.38*	*7.20*	*b.d.l.*	*0.01*	*17.34*	*24.27*	*0.38*	*0.01*	*0.00*	*0.97*	*1.07*	*0.99*

analyses results are given in mass% (except for cation numbers)

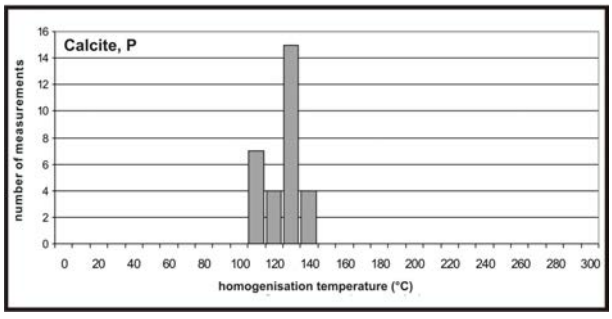

Figure 3. Frequency distribution diagram of homogenisation temperatures measured in primary inclusions of the calcite from the cooling cracks of basalt.

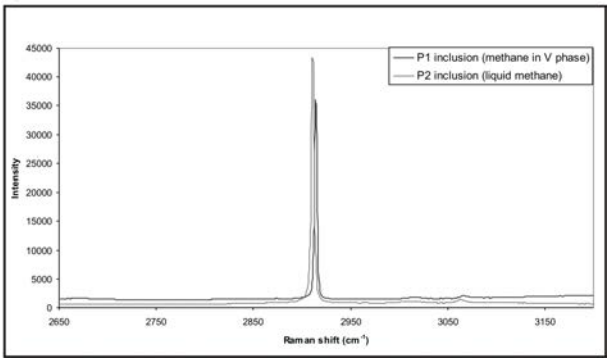

Figure 4. Methane peaks in the Raman spectra of the vapour phase in a P1 type inclusion and the liquid phase of a P2 inclusion in datolite. The slight decrease of Raman shift in the case of P2 inclusion is due to the higher density of liquid methane.

as well. The volume of vapour phase in these inclusions appears to be fairly constant at around 5-10% at room temperature. Homogenisation temperatures for those primary fluid inclusions (T_h(LV→L)) are between 118 and 143°C (Fig. 3, Table 3). Eutectic temperatures are around -21°C, indicating NaCl-H_2O composition. Salinities calculated on the basis of the observed ice melting temperatures range from 4.95 to 9.07 NaCl equiv. mass% (Table 3). Fracture/cleavage plane related secondary inclusions of calcite are much smaller (<10 μm) than the primary ones. They usually contain liquid aqueous phase on room temperature; a few liquid and vapour phase bearing inclusions among the monophase ones suggest to post entrapment necking down. Fluid inclusion microthermometry was not perfomed in secondary inclusions of calcite.

From the cross-cutting type, more extended veins, fluid inclusion studies have been performed in datolite, as prehnite is not a good host for fluid inclusions (it contains lamellae of cleavage planes and crystals are strained), whereas the rare calcite and quartz in these veins do not contain fluid inclusions large enough for reproducible microthermometry.

The primary fluid inclusion assemblage of datolite is characterized by two end members according to their phase compositions at room temperature: aqueous liquid rich, methane bubble bearing (L_{aq}+V_{CH4}) inclusions (P1) with variable, 5-25 vol. % vapour phase content and liquid methane rich (L_{CH4}) inclusions (P2), with no visible aqueous liquid phase. Typical sizes of P1 inclusions are between 5 and 20 μm whereas P2 inclusions attain sizes up to 30 μm. These primary fluid inclusions occur in "clouds", apart from the healed microfractures of the host crystals, (mainly in spongy and transitional datolites) and isolated (mainly in water-clear datolites) (Fig. 2**F**, **G**). Inclusions in the spongy datolite are extremely abundant and their sizes are well below 10 μm. Observations were largely obscured by the abundance of liquid methane rich P2 type inclusions with dark outline, but a few aqueous liquid rich P1 inclusions with variable vapour phase volumes were also detected in that variety of datolite.

Methane content of the vapour phase of the P1 aqueous inclusions was proven by high resolution Raman spectroscopy at room temperature (Fig. 4). No trace of other gas component was detected. In the homogenized P1 inclusions no methane peak could be observed in the Raman spectra; this behaviour suggests that the amount of methane is very small in these inclusions (i.e. below 0.01 m, [32]) (Fig. 5**A**).

P1 inclusions in spongy datolite showed the lowest homogenisation temperatures (T_h(LV→L)=160-252°C) whereas they provided the highest homogenisation temperatures (T_h(LV→L)=209-264°C) in the water-clear crystals. P1 inclusions in datolites of transitional appearance are characterised with homogenisation temperatures between the two above mentioned ranges; in the more spongy ones, P1 inclusions have lower homogenization temperatures (T_h(LV→L)=182-262°C), whereas the more clear types homogenise at slightly higher temperatures (T_h(LV→L)=191-275°C (Fig. 6**A**-**D**, Table 3). The eutectic temperatures observed during the freezing studies were -21.4°C+/-0.6°C, suggesting a NaCl-H_2O composition of the aqueuos phase. Ice melting temperatures ranged from -0.1°C to -1.1°C. Formation of methane-clathrate was not observed during the freezing studies, therefore salinities from 0.18 to 1.9 NaCl equiv. mass % [23] were estimated on the basis of ice melting temperatures. The calculated salinities are quite similar in every types of datolite (Table 3). Salinities of some of these aqueous inclusions were also calculated using Raman spectroscopy. Though a more recent calculation method is known (e.g. [33]), here the older method of [34] was used, as the cited new method

Table 3. Results of the fluid inclusion microthermometry.

	Inclusion type	Number of measurements	Min. Th	Max. Th	Min. Te	Max. Te	Min. Tmice	Max. Tmice	Min. salinity	Max. salinity
Spongy datolite	P1, $L_{aq}+V_{CH4}$	25	160.0	252.0	–	–	-0.7	-0.2	0.35	1.22
Spongy-transitional datolite	P1, $L_{aq}+V_{CH4}$	16	182.0	262.0	-20.9	–	-0.5	-0.1	0.18	0.88
Spongy-transitional datolite	P2, L_{CH4}	3	-84.5	-83.3	–	–	–	–	–	–
Water-clear-transitional datolite	P1, $L_{aq}+V_{CH4}$	27	191.0	275.0	-22.1	-21.5	-0.8	-0.1	0.18	1.4
Water-clear-transitional datolite	P2, L_{CH4}	14	-90.6	-83.8	–	–	–	–	–	–
Water-clear-transitional datolite	S1, $L_{aq}+V_{CH4}$	4	146.0	178.0	–	–	-0.6	-0.4	0.92	1.05
Water-clear datolite	P1, $L_{aq}+V_{CH4}$	15	209.0	264.0	-20.9	-20.5	-0.8	-0.1	0.18	1.4
Water-clear datolite	P2, L_{CH4}	15	-91.0	-85.2	–	–	–	–	–	–
Water-clear datolite	S2, L_{CH4}	9	-86.9	-83.5	–	–	–	–	–	–
Water-clear datolite	S3, L_{CH4}	9	-95.0	-94.0	–	–	–	–	–	–
Calcite in cooling cracks	P, L+V	30	118.0	143.0	-22.5	-20.9	-5.9	-3.0	4.95	9.07

Temperatures are given in °C.

Salinities are given in NaCl equiv. mass%

was developed in quartz and requires special orientation of the laser polarisation plane in order to eliminate the effect of the birefrigence of the mineral. The calculation was done using the method of [34], which is based on the integrals of the peak areas between 2900-3300 cm^{-1} (X) and 3300-3700 cm^{-1} (Y) (Table 4). The effect of birefringence was decreased with measuring inclusions in increased depth, according to the suggestion of [33]. Because the OH-peak of datolite is also in this range, not only the background, but also the datolite OH peak measured in an inclusion-free area was substracted -after normalization to equal intensity- from the results of measurements performed in the fluid inclusions (Fig. 5**B**). After correction, salinities from 1.12 to 1.25 NaCl equiv. mass % were obtained for the inclusions. These data are in a very good agreement with salinities calculated from ice melting temperatures of the same inclusions (Table 4).

In P2 inclusions, a vapour bubble appeared upon cooling at about -95°C. The homogenisation temperature of these inclusions showed a gradual change from the transitional (T_h(LV→L) = -90.6 to -83.3°C) to the water-clear (T_h(LV→L) = -91.5 to -85.2°C) datolite (Table 3, Fig. 7**A**-**B**). No freezing of P2 inclusions was observed during cooling down to -180°C temperature. Methane content of these inclusions was also confirmed by Raman spectroscopy; the slight decrease in Raman shift (2911-2912 cm^{-1}) in comparison to the gas phase of P1 inclusions is due to the higher density of methane liquid. Other components were not identified in these inclusions at room temperature (Fig. 4). The optically invisible water content of carbonic fluid inclusions can be detected by Raman spectroscopy if the inclusion is heated up to bulk homogenisation temperature [35]. However, no trace of water was detectable at temperatures up to 180-250°C; i.e. the range of homogenization temperatures of P1 type primary fluid inclusions.

At least three generations of secondary inclusions were observed in datolite; S1 is an aqueous liquid phase rich inclusion with around 5 vol. % methane bearing vapour phase ($L_{aq}+V_{CH4}$), while S2 and S3 are liquid methane

Table 4. Salinity calculations.

		Microthermometry		Raman spectroscopy			
Sample	Number of inclusions	Minimum salinity	Maximum salinity	minimum (Y-X)/((X+Y)/2)	maximum (Y-X)/((X+Y)/2)	Minimum salinity	Maximum salinity
Spongy-transitional datolite	7	0.88	1.22	0.50	0.582	1.12	1.23
Water-clear-transitional datolite	7	1.05	1.4	0.524	0.540	1.20	1.25

salinity is given in NaCl equiv. mass%

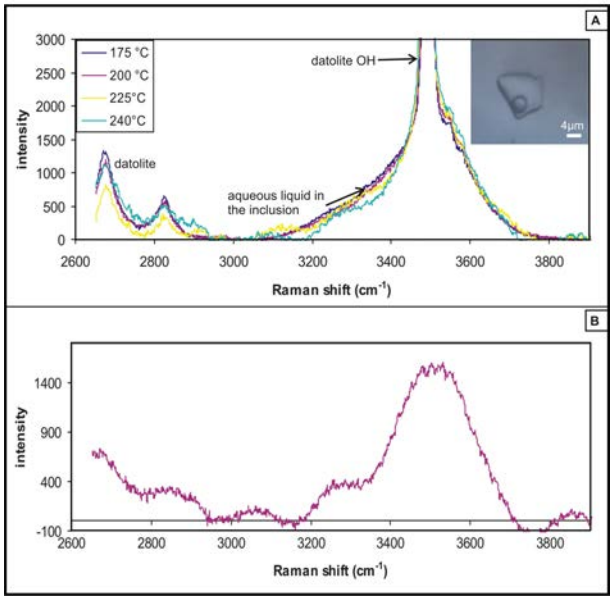

Figure 5. Raman spectra of a P1 inclusion in datolite upon heating. **A** No methane peak at ~2917 cm^{-1} Raman shift is detected in the homogenised inclusion. **B** Raman spectra of a P1 type inclusion of datolite after intensity normalization and substraction of the OH-peak of datolite and the background.

bearing inclusions with no visible aqueous liquid phase (L_{CH4}) (Fig. 2F, G). The size of the S1 inclusions is 10-30μm, while S2 and S3 were smaller, generally below 10μm. These inclusions were found in healed microcracks in different datolite types (transitional and water-clear). In transitional type datolite only S1 inclusions occur, while in water clear datolites no aqueous liquid rich inclusions were found. It is therefore likely they do not belong to the same fluid inclusion assemblage. In analogy to the primary inclusions, only methane was detected by Raman spectroscopy in the vapour phase of the S1 and also in the liquid phase of the S2 and S3 inclusions. The homogenisation temperatures (T_h(LV→L)) in S1 inclusions range from 146 to 178°C (Table 3). This is slightly lower and overlaps with the lowest (T_h(LV→L)) temperatures of P1 fluid inclusions. Methane in S2 inclusions homogenized into the liquid phase between -86.9 and -83.5°C and in S3 inclusions between -95.0 and -94.0°C (Table 3). Thus, secondary methane rich inclusion generations also have different homoegnisation temperatures in comparison to the primary ones.

5. Discussion

The observed phase compositions of primary fluid inclusions in calcite from the cooling cracks of basalt suggest a homogeneous parent fluid, thus homogenisation temperature data need pressure correction. Composition of chlorite may be used as temperature indicator of mineral forming processes [36–38]. This was shown earlier in the studied area by [39], using the method of [38]. However, chlorite composition, structure and crystallite size was studied by [40, 41] in the area, and differences were found according to the change in the metamorphic grade. In our case, the measured compositions of chlorite lie within the required range of [36], resulting crystallisation temperature of the chlorite-calcite cooling crack assemblage is around 160°C, while for the matrix chlorite an average temperature of 177°C is calculated (Table 1). As this chlorite thermometer has an uncertainity of around 20°C [36], the results show also a slight scattering between 171-192°C, but their average is obviously slightly higher than in the cooling cracks. This temperature difference may be attributed to the very rapid cooling of the system during the lava-water interaction. These temperatures correspond to 0.5-0.6 kbar pressure along the isochor calculated from average homogenization temperature and salinity data for primary inclusions of calcite. This suggests that the submarine hydrothermal activity has taken place at about 5-6 km water depth during cooling of the basalt,

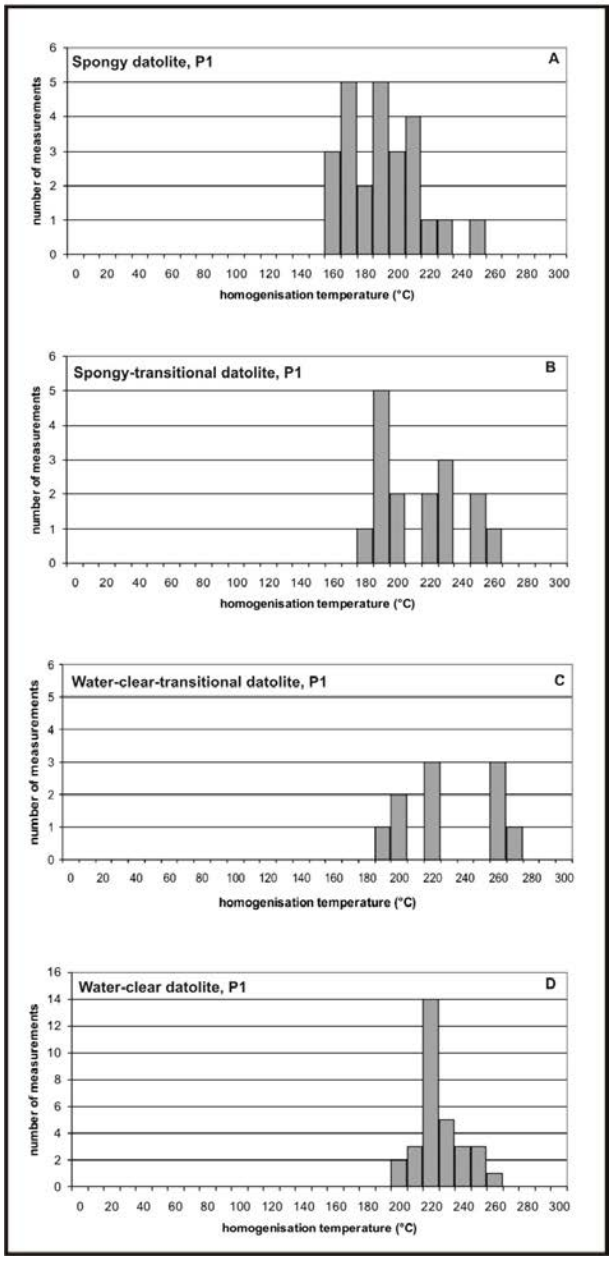

Figure 6. Frequency distribution of homogenisation temperatures measured in P1 inclusions of datolite (**A** spongy datolite **B** spongy-transitional datolite **C** water-clear transitional datolite **D** water-clear datoltie).

in accordance with the proposed geological setting for the submarine volcanism. The slightly higher salinities compared to the seawater could have been caused by the seawater-rock interaction, i.e. the growth of secondary, water-bearing minerals in the basalt results in increase of salt concentration of the parent fluid [42].

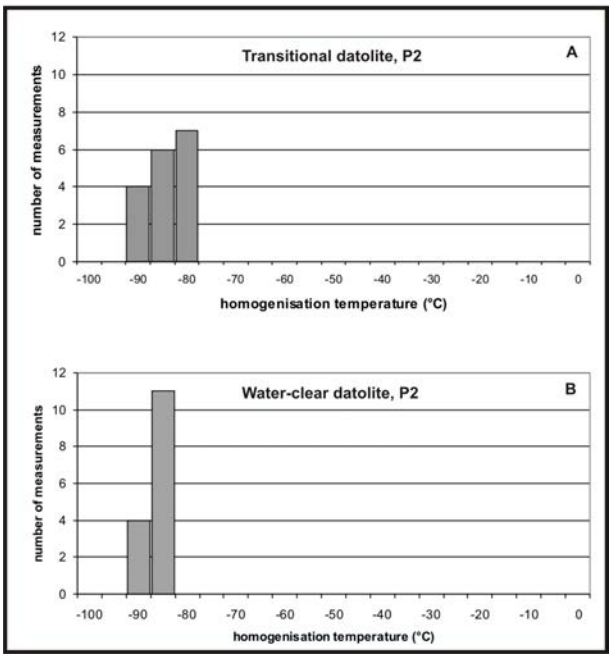

Figure 7. Frequency distribution of homogenisation temperatures measured in P2 inclusions of datolite (**A** transitional datolite **B** water-clear datolite).

Fluid inclusion petrography suggests that datolite from the hydrothermal veins cutting the mineralized cooling cracks of basalt crystallised from a heterogeneous fluid system. Generally, the solubility of methane into water and *vice versa* is relatively low, so it is common to reach saturation with respect to the aqueous phase, especially under low pressure conditions. Therefore, the entrapment of fluid inclusions in an immiscible system results in two end-member, methane rich and a water rich inclusions [43]. In this case, the minimum homogenisation temperatures obtained from the primary aqueous liquid rich (i.e. P1 type) inclusions corresponds to the entrapment and crystallisation temperature. Thus, the crystallisation temperature for the spongy datolite is around 160°C, for the spongy-transitional one is around 180°C, whereas the water-clear-transitional datolite precipitated at around 190°C and the water-clear crystals at around 210°C (see Table 3). The salinity of aqueous parent fluid was rather low, between 0.18-1.9 NaCl equiv. mass % (Fig. 8). The low chlorine content of the parent fluid system may explain the Cl-poor composition of datolite too, however, it is definitely lower than those of found in the submarine hydrothermal process related cooling cracks' calcites.

The water-clear datolite is also associated with chlorite. The XFe=0.45-0.49 and Al(IV)=0.98-1.05 composition of

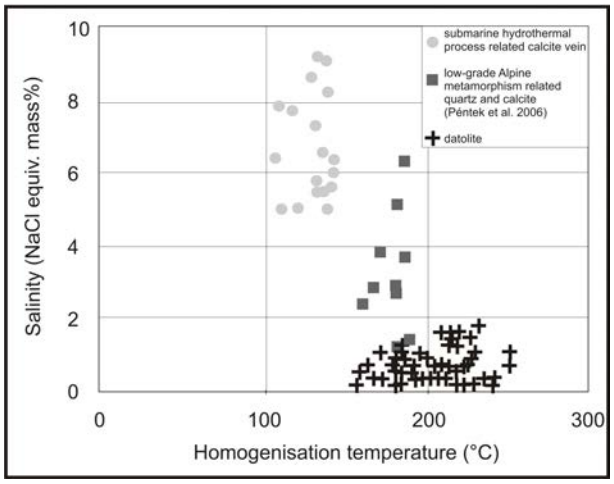

Figure 8. Homogenisation temperature vs. salinity discrimination diagram for fluid inclusions entrapped during the submarine hydrothermal and Alpine metamorphic processes in the Szarvaskő Unit (the latter determined by [22]).

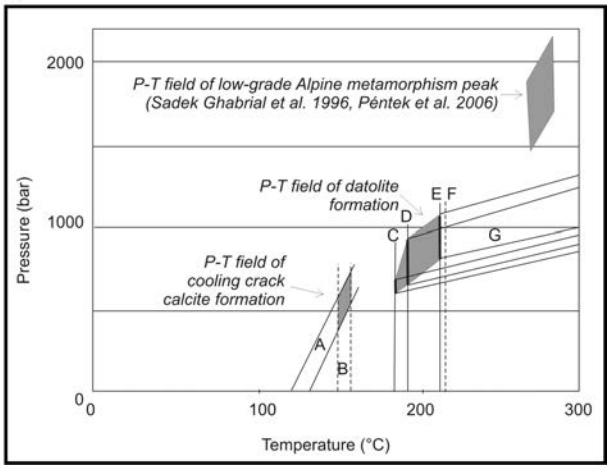

Figure 9. Entrapment conditions (p-T) of primary fluid inclusions of calcite from the cooling cracks of basalt, datolite from cross cutting veins and Alpine peak-metamorphism related veins in the Szarvaskő Unit. The peak metamorphic conditions were previously determined in [22, 45]. Entrapment conditions were determined by using the isochores calculated from the homogenisation temperatures of cooling cracks' calcite **(A)**, formation temperature got from chlorite thermometry **(B, F)**, minimum homogenisation temperature of spongy-transitional **(C)**, water-clear-transitional **(D)** and water-clear datolite **(E)** and corresponding isochors of the methane-bearing inclusions **(G)**.

that type of chlorite is compatible with the calibration of [36], resulting in an average chlorite formation temperature of 220°C (Table 1). There is a remarkable agreement (i.e. within the uncertainity of the method) between the crystallisation temperature for water-clear datolite and the synchronously precipitated chlorite. This supports the view that the minima of homogenization temperatures for the primary aqueous inclusions indeed correspond to the true temperatures of parent fluids of various datolite generations. Thus the fluid inclusion data suggest that a continuous increase of temperature has occured during the precipitation of datolite, from the spongy to the water-clear types.

The P1 inclusions of datolite also contain a small amount of methane as vapour phase, as shown by Raman spectroscopy. The P2 type primary inclusions, the methane rich counterparts of the P1 type inclusions may also contain a very small amount of aqueous phase wetting the wall of the inclusions, indetectable by high resolution Raman spectroscopy. Therefore we assume very low water contents of P2 type inclusions, thus their compositions may be well modelled in the pure CH_4 system. The trapping pressures of primary fluid inclusion generations are estimated by pressures along P2 inclusions' isochores corresponding to the minimum homogenization temperatures of P1 type inclusions. Though the presence of certain amount of water below the detection limit of the Raman spectroscopy may slightly modify the isochore of P2 inclusions, this effect is geologically negligible (i.e. at ~220°C temperature and <1 kbar pressure a possible shift to higher pressures is about 15 bar – if phase equilibrium is assumed, inside the immiscibility field at the given P-T – [44]).

Following the procedure described above, crystallisation pressures were determined for the spongy-transitional, water-clear-transitional and transitional datolites only, as no measurable primary methane inclusions (P2) were found in the spongy datolite. A gradual increase of pressure was found from the spongy-transitional (0.6-0.7 kbar) through the water-clear-transitional (0.7-0.9 kbar) to the water-clear (0.8-1.1 kbar) crystals (Fig. 9).

As no acqueous inclusions were found in association to the secondary S2 and S3 methane inclusions, no pressure was determined for their entrapment conditions. However, it can be assumed that methane-bearing fluids were migrated in the semi-closed drusy veins after the crystallization of datolite.

Entrapment temperature and pressure, chemical and phase composition, as well as salinity data for primary fluid inclusions clearly demonstrate that datolite crystallization cannot be related to submarine hydrothermal processes at the studied locality (Fig. 8. 9). This is also indicated by the presence of a hydrothermal alteration halo around datolite bearing veins: the parent fluid of the datolite bearing mineral assemblage was not in equilibria with the basalt altered by submarine hydrothermal processes.

A mineral assemblage similar to the investigated datolite bearing veins (containing prehnite, chlorite, quartz, calcite, albite) was reported in some very low-grade Alpine metamorphism-related veins in the gabbro of the Szarvaskő Unit [2, 13, 22, 45]. According to these results, a maximum formation temperature and pressure condition for the vein filling minerals in the SW Bükk Mts. was found to be 270-285°C and 1.5-2 kbar. Thus datolite formed before the peak of the Alpine metamorphism, under the increasing temperature-pressure conditions of prograde metamorphism (Fig. 9).

The individual datolite crystals show gradual textural change, formation temperature and pressure increase suggesting that the crystal precipitation was not a continuous process; a step-by-step mechanism is more probable. Thus a single vein comprising of these datolites can represent a longer episode of the progressive metamorphism.

Since the only known locality of datolite in the Szarvaskő Unit is the siliciclastic peperitic facies of the Egerbakta quarry, the presence of admixed sedimentary rock in the basalt seems to be an important factor. Probably, the source of boron was the (now completely altered) sediment of the locally occurring peperitic facies. However, in case of methane also an external source might be possible.

Though the very low-grade Alpine metamorphism is a regional event, datolite-bearing veins are found only locally. Thus during the first steps of this process, the fluids were generated mostly by dehydration of the admixed sediment, while the alteration products of basalt were not as dominant and these fluids flew only in some particular cracks.

Euhedral datolite bearing veins were also found at some pillow basalt and rarely gabbro localities in the Mesozoic ophiolites of the Northern-Appenines, Italy [46]. Though no methane was found in primary fluid inclusions at this locality, they do contain CO_2. Similarly to the datolites of Egerbakta, the origin of datolite may also be related to processes superimposing the submarine hydrothermal alteration.

6. Conclusions

Based upon investigations of datolite associated with Jurassic pillow basalts in the Szarvaskő Unit of the Bükk Mts., northeastern Hungary, the effects of cooling-related submarine hydrothermal and very low-grade Alpine metamorphic processes were recognised. The short, thin veinlets filled by calcite with minor quartz, prehnite and chlorite in the cooling cracks of pillows are related to hydrothermal alteration which took place under conditions of 160-170°C temperature and 0.5-0.6 kbar pressure (corresponding to 5-6 km water depth). The elevated salinities (5-9 NaCl equiv. mass %) suggest to modification of sea water composition due to formation of water bearing alteration minerals at low water/rock ratios in the limited pore spaces and wall rock of the thin and short cooling cracks. The datolite, prehnite, quartz, calcite and albite bearing veins are associated with the progression of the very low-grade Alpine metamorphism at increasing temperature from 160°C to 210°C and pressure from 0.6 kbar to 1.1 kbar. The investigated datolite precipitated from low-salinity (0.2-2 NaCl equiv. mass %), methane-bearing heterogenous fluids in those parts of the basaltic blocks where sediments are admixed to the volcanic rock. Our results also confirmed that salinity calculations based on the Raman spectra of aqueous inclusions and chlorite thermometry are useful tools in understanding mineral forming processes in low temperature open systems.

Acknowledgements

This work was supported by the Baross Gábor Program of the National Research and Technology Agency (NKTH), Hungary. The University Centrum for Applied Geosciences (UCAG) is thanked for the access to the E. F. Stumpfl Electron Microprobe Laboratory. The authors give thanks to reviewers for their useful comments which helped a lot in the improvement of the manuscript.

References

[1] Kiss G., Molnár F., Koller F., Péntek A., Triassic rifting and Jurassic ophiolite-like magmatic rocks in the Bükk Unit, NE-Hungary –an overview. *Mitteilungen der Österreichischen Mineralogischen Gesellschaft*, 2011, 157, 43-69

[2] Árkai P., Very low- and low-grade Alpine regional metamorphism of the Paleozoic and Mesozoic formations of the Bükkium, NE Hungary. *Acta Geologica Hungarica*, 1983, 26, 83-101

[3] Árkai P., Balogh K., Dunkl I., Timing of low-temperature metamorphism and cooling of the Paleozoic and Mesozoic formations of the Bükkium, innermost western Carpathians, Hungary. *Geol. Rundsch.*, 1995, 84, 334-344

[4] Árkai P., Alpine regional metamorphism in the main tectonic units of Hungary: a review. *Acta Geologica Hungarica*, 2001, 44, 329-344

[5] Szakáll S., Gatter I., Szendrei G., A magyarországi ásványfajok (*Minerals of Hungary*). Kőország Kiadó, 2005, Budapest

[6] Grew E. S., Borosilicates (exclusive of tourmaline)

and boron in rockforming minerals in metamorphic anvironments. In: Grew E.S., Anovitz L.M. (Eds.): Boron mineralogy, petrology and geochemistry. *Reviews Mineral.*, 1996, 33, 387-502

[7] Gaines R.V., Skinner H.C.W., Foord E.E. Mason B., Rosenzweig A., Dana's New Mineralogy. 8th edition, John Wiley and Sons Inc, 1997

[8] Csontos L., A Bükk hegység mezozoós rétegtani újraértékelése [Re-evaluation of the Mesozoic stratigraphy of the Bükk Mts.]. *Földani Közlöny*, 2000, 130, 95-131

[9] Haas J., Kovács S., The Dinaric-Alpine connection – as seen from Hungary. *Acta Geologica Hungarica*, 2001, 4, 345-362

[10] Kovács S., Haas J., Szebényi G., Gulácsi Z., Pelikán P., B.-Árgyelán G., Józsa S., Görög Á., Ozsvárt P., Gecse Zs., Szabó I., Permo-Mesozoic formations of the Recsk-Darnó Hill area: stratigraphy and structure of the pre-tertiary basement of the paleogene Recsk orefield. In: Földessy J., Hartai É. (Eds.): Recsk and Lahóca Geology of the Paleogene Ore Complex. Geosciences, Publications of the University of Miskolc, Series A, Mining, 2008, 73, 33-56

[11] Szentpéteri Zs., Diabase and gabbro bodies in Southern Bükk. *Magyar Állami Földtani Intézet Évkönyve*, 1953, 41, 3-102

[12] Balla Z., The North Hungarian Mesozoic mafics and ultramafics. *Acta Geologica Hungarica*, 1984, 27, 341-357

[13] Sadek Ghabrial D., Árkai P., Magmatic features and metamorphism of plagiogranite associated with a Jurassic MORB-like basic-ultrabasic complex, Bükk Mountains, Hungary. *Acta Petrologica et Mineralogica*, 1994, 35, 41-69.

[14] Kubovics I., Szabó Cs., Harangi Sz., Józsa S., Petrology and petrochemistry of Mesozoic magmatic suites in Hungary and adjacent areas: An overview. *Acta Geodaetica et Geophysica Hungarica*, 1990, 25, 345-371

[15] Downes H., Pantó G., Ärkai P., Thirlwall M. F., Petrology and geochemistry of Mesozoic igneous rocks, Bükk Mountains, Hungary. *Lithos*, 1990, 24, 201-215

[16] Harangi Sz., Szabó Cs., Józsa S., Szoldán Zs., Árva-Sós E., Balla M., Kubovics I., Mesozoic igneous suites in Hungary: Implications for genesis and tectonic setting in the northwestern part of Tethys. Internat. *Geol. Review.*, 1996, 38, 336-360

[17] Aigner-Torres M., Koller F., Nature of the magma source of the Szarvaskő complex (NE-Hungary). Ofioliti, 1999, 24, 1-12

[18] Pamić J., Tomljenović B., Balen D., Geodynamic and petrogenetic evolution of Alpine ophiolites from the central and NW Dinarides: an overview. *Lithos*, 2002, 65, 113-142

[19] Csontos L., Vörös A., Mesozoic plate tectonic reconstruction of the Carpathian region. *Palaeogeogr. Palaecol.*, 2004, 210, 1– 56

[20] Árváné Sós E., Balogh K., Ravaszné Baranyai L., Ravasz Cs., Mezozoós magmás kőzetek K/Ar kora Magyarország egyes területein [K/Ar ages of the Mesozoic magmatic rocks from different localities of Hungary]. MÁFI Évi Jelentése az 1985. évről, MÁFI, Budapest, 1987, 295-307

[21] Pamić J., Gušić I., Jelaska V., Geodynamic evolution of the Central Dinarides. *Tectonophysics*, 1998, 297, 251-268

[22] Péntek A., Molnár F., Watkinson D. H., Magmatic fluid segregation and overprinting hydrothermal processes in gabbro pegmatites of the Neotethyan ophiolitic Szarvaskő Complex (Bükk Mountains, NE Hungary). *Geol. Carpath.*, 2006, 57, 433-446

[23] Hall D.L., Sterner S. M., Bodnar R. J., Freezing point depression of NaCl-KCl-H_2O solutions. *Econ. Geol.*, 1988, 83, 197–202

[24] Naden J., CalcicBrine; a Microsoft Excel 5.0 add-in for calculating salinities from microthermometric data in the system NaCl-$CaCl_2$-H_2O. In: Brown P. E., Hagemann S. G. (Eds.) PACROFI VI, Madison, WI., 1996

[25] Potter R.W., Clynne M.A., Solubility of highly soluble salts in aqueous media - Part I. NaCl, KCl, $CaCl_2$, Na_2S0_4 and K_2S0_4 solubilities to 100°C. Journal of Research of the U. S. Geological Survey, 1978, 6, 701-705

[26] Zhang Y. G., Frantz J. D., Determination of homogenization temperatures and densities of supercritical fluids in the system NaCl-KCl-$CaCl_2$-H_2O using synthetic fluid inclusions. *Chem. Geol.*, 1987, 64, 335-350

[27] Holloway J.R., Compositions and volumes of supercritical fluids in the earth's crust. In: Hollister L. S., Crawford M. L. (Eds.), MAC Short Course in Fluid Inclusions. Mineral Association of Canada,1981, 6, 13-38

[28] Brown P.E., FLINCOR; a microcomputer program for the reduction and investigation of fluid-inclusion data. *Am. Mineralogist*, 1989, 74/, 1390-1393

[29] Bakker R. J., Package FLUIDS 1. Computer programs for analysis of fluid inclusion data and for modelling bulk fluid properties. *Chem. Geol.*, 2003, 194, 3-23.

[30] Zane A., Weiss Z., A procedure for classifying rock-forming chlorites based on microprobe data. Rendiconti Lincei Scienze Fisiche e Naturali, serie 9, 1998,

9, 51-56
[31] Palache C., The minerals of Franklin and Sterling Hill, Sussex County, New Jersey. USGS Professional Paper, 1935
[32] Dubessy J., Buschaert S., Lamb W., Pironon J., Thiéry R., Methane bearing aqueous fluid inclusions: Raman analyses, thermodynamic modelling and application to petroleum basins. *Chem. Geol.*, 2001, 173, 193-205
[33] Baumgartner M., Bakker R. J., Raman spectroscopy of pure H_2O and NaCl-H_2O containing synthetic fluid inclusions in quartz—a study of polarization effects. *Mineral. Petrol.*, 2009, 95, 1-15
[34] Mernagh T. P., Wilde A. R., The use of the Raman microprobe for the determination of salinity in fluid inclusions. *Geochim. Cosmochim. Acta*, 1989, 53, 765–771
[35] Tsunogae T., Dubessy J., Ethane- and hydrogen-bearing carbonic fluid inclusions in a high-grade metamorphic rock. *J. Mineral. Petrol. Sci.*, 2009, 104, 324-329
[36] Zang W., Fyfe W. S., Chloritization of the hydrothermally altered bedrock at the Igarapé Bahia gold deposit, Carajás, Brazil. *Mineral. Deposita*, 1995, 30, 30-38
[37] Kranidiotis P., MacLean W. H., Systematics of chlorite alteration at the Phelps Dodge massive sulfide deposit, Matagami, Quebec. *Econ. Geol.*, 1987, 82, 1898-1911
[38] Cathelineau M., Izquierdo G., Temperature — composition relationships of authigenic micaceous minerals in the Los Azufres geothermal system. *Contrib. Mineral. Petrol.*, 1988, 100, 418-428
[39] Árkai P., Sadek Ghabrial D., Chlorite crystallinity as an indicator of metamorphic grade of low-temperature meta-igneous rocks: A case study from the Bükk Mountains, Northeast Hungary. *Clay. Min.*,1997, 32, 205-222
[40] Árkai P., Mata M. P., Giorgetti G., Peacor D. R., Tóth M., Comparison of diagenetic and low-grade metamorphic evolution of chlorite in associated metapelites and metabasites: an integrated TEM and XRD study. *J. Metamorph. Geol.*, 2000, 18, 531-550
[41] Mata M. P., Giorgetti G., Árkai P., Peacor D. R., Comparison of evolution of trioctahedral chlorite/berthierine/smectite in coeval metabasites and metapelites from diagenetic to epizonal grades. *Clays Clay Min.*, 2001, 49, 318-332
[42] Nehlig P., Salinity of oceanic hydrothermal fluids: a fluid inclusion study. *Earth and Planet. Sci. Letters*, 1991, 102, 310-325
[43] Goldstein R. H., Fluid inclusions in sedimentary and diagenetic systems. *Lithos*, 2001, 55, 159-193
[44] Hurai V., Fluid inclusion geobarometry: pressure corrections for immiscible H_2O-CH_4 and H_2O-CO_2 fluids. *Chem. Geol.*, 2010, 278, 201-211
[45] Sadek Ghabrial D., Árkai P., Nagy G., Alpine polyphase metamorphism of the ophiolitic Szarvaskő Complex, Bükk Mountains, Hungary. *Acta Mineral. Petrol.*, 1996, 37, 99-128
[46] Zaccarini F., Morales-Ruano S., Scacchetti M., Garuti G., Investigation of datolite ($CaBSiO_4OH$) from basalts in the northern Apennines ophiolites (Italy): genetic implications. Chemie der Erde - Geochemie, 2008, 68, 265-277